

11-1-93  
201704  
15 P

**Technical Status Report**  
**for Effort Entitled**  
**"New Concepts for HgI<sub>2</sub> Scintillator**  
**Gamma Ray Spectroscopy"**

**Contract NAS7-1204**

**For the Period September 1, 1993**  
**through November 30, 1993**

**Submitted By:**  
**Jan S. Iwanczyk, Ph.D.**  
**Principal Investigator**  
**Xsirius, Inc.**  
**1220 Avenida Acaso**  
**Camarillo, CA 93012**  
**(805) 484-8300**

**Submitted To:**  
**G. Veronica Stickley, Contracting Officer**  
**Gordon S. Chapman, NASA Technical Monitor, Code SJT**  
**Dr. Patricia McGuire, JPL Manager SBIR Program, M/S 79/21**  
**Dr. Albert E. Metzger, JPL Technical Monitor, M/S 183-501**  
**NASA Resident Office - Jet Propulsion Laboratory**  
**4800 Oak Grove Drive**  
**Pasadena, CA 91109**

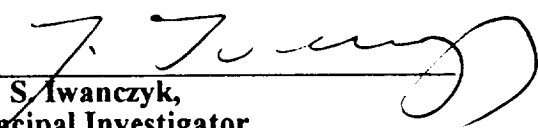
**DCMAO, Van Nuys**  
**6230 Van Nuys Blvd.**  
**Van Nuys, CA 91401**

(NASA-CR-194819) NEW CONCEPTS FOR  
HG12 SCINTILLATOR GAMMA RAY  
SPECTROSCOPY Technical Status  
Report, 1 Sep. - 30 Nov. 1993  
(Xsirius Scientific) 15 p

N94-24113

Unclass

G3/25 0201704

By:   
Jan S. Iwanczyk,  
Principal Investigator

Date: 01/14/94

FIFTH QUARTER TECHNICAL STATUS REPORT OF  
"NEW CONCEPTS FOR HgI<sub>2</sub> - SCINTILLATOR GAMMA RAY SPECTROSCOPY"  
CONTRACT # NAS7-1204  
FOR THE PERIOD ENDING NOVEMBER 30, 1993

Our primary goals in this project are development of the technology for HgI<sub>2</sub> photodetectors (PD's), development of HgI<sub>2</sub>/scintillator gamma detector, development of electronics, and finally development for a prototype gamma spectrometer. The milestones for attaining these goals are shown in Table I. Each of the subtopics below addresses one of the milestones and describes our progress towards achieving them. We have not deviated from the proposed schedule, and are generally on target for each line item.

(1) Development of HgI<sub>2</sub> PD's (on schedule)

a) HgI<sub>2</sub> purification and crystal growth (complete - refer to original two year schedule, Table I)

During the first six months of the project, the main effort was focused on crystal growth and adjustment and refinement of the purification process to achieve optimized electrical parameters for PD operation. To evaluate the purity level of our output material from each purification step, the samples were collected and sent to Sandia National Laboratory for chemical analysis. Test detectors were made out of each crystal grown in our lab. The electrical parameters, which include  $\mu\tau$  for electrons, energy resolution, leakage current and detector stability were measured. After satisfactory electrical parameters of crystals were obtained, the effort shifted toward growing large volume crystals necessary for fabrication of large-area PD's. Several crystals big enough to make PD's of 1" diameter or larger have been grown. A one inch detector has been fabricated from one of our crystals. This detector has shown stable performance with an energy resolution of 7.4% FWHM at 662 keV. We have identified where improvements can be made in the preparation of the hydrogel contact to reduce inclusions of air bubbles that lead to poor light collection and hence deteriorated energy resolution. This detector will be refabricated using this method and we hope to get improved results. More PD's will be fabricated out of our own crystals.

In addition to the emphasis on growing large bulk crystals, large-area, flat "pancake" shaped crystals were grown. Historically, HgI<sub>2</sub> crystal shape has been tailored to production of volumetric (cube shaped) detectors for gamma-ray spectroscopy. We are developing new techniques to produce crystals better suited to the PD geometry by changing the orientation of the growing crystal to force a "pancake" shape. Using this method, larger areas can be grown in a shorter period and the crystal can be used more efficiently for large-area PD fabrication. The first two pancake shaped crystals grown in our lab have been fabricated into 1" diameter PD's. We are encouraged by the results; however, the crystal growth conditions for this new technique still need to be optimized. Some non-uniformities were found in these first two pieces of "pancake" shaped crystals and the two PD's made from these crystals did not work satisfactorily. Two new

"pancake" shaped crystals have been grown. They appear more uniform than the first two crystals. PD's will be fabricated and tested from the new crystals.

#### b) Surface and contact studies

Preparation of the detector surface is an important factor directly affecting PD performance. The absorption depth of the scintillation light in  $\text{HgI}_2$  is only a few microns; therefore, the collection of free charge carriers generated by the absorbed photons is decreased by both surface recombination and bulk trapping. The detectors are always operated with a negative polarity on the irradiation electrode so that the signal currents are almost entirely carried by electrons. For electrons the surface recombination dominates the charge collection. Since electron bulk trapping is relatively negligible, an improvement in detector performance can be achieved by optimizing surface preparation procedures and by incorporating electrode technology which reduces the surface recombination velocities.

We have shown that hydrogel is a good material for the entrance electrode of the PD. However, the parameters of the material vary from batch to batch and hence affect the detector performance. Some comparison measurements on the hydrogel have been performed. First, we made a PD using the hydrogel from one batch and tested it. Then, we refabricated the detector using the hydrogel from another batch and tested again. These comparison measurements were repeated with a group of five crystals. The results showed that detectors made from the first batch of the hydrogel all performed very well in terms of energy resolution and stability. The detectors made from the second batch showed bad resolution or had a deteriorated response with time. Samples from these two batches of hydrogel have been sent to Sandia National Laboratory to be chemically analyzed. At the same time we are planning to make a hydrogel-like material in our own lab. This will make it easier to control the material parameters. This is further necessitated because the Promeon Company, which made the hydrogel for us in the past as a special custom ordered material, is no longer making the type of hydrogel suitable for high quality PD's.

Another medical coupling gel was also experimentally tested for the detector entrance electrode. This gel is an aqueous conductive coupling agent for medical electrosurgery. It appears water clear and is electrically conductive. Two 0.5" PD's were made using this material as the entrance electrode. The first one had a very simple structure and was not encapsulated. The FWHM energy resolution for 662 keV gamma-ray of this detector was 5.2%. However, the gel deteriorated when it was exposed to the air for the period of one or two days. The second detector that was fabricated with the gel contained a Teflon ring and was sealed with Humiseal. The gel remained clear and transparent and did not show any reaction with the  $\text{HgI}_2$  crystal after a few weeks. A good photopeak was obtained at the beginning; however, it deteriorated over time. Further experiments are planned with this contact material.

#### c) PD structure optimization

The guard ring configuration that we developed for the PD's has proved to be a good structure to reduce surface leakage currents and resulting associated electronic noise. This

configuration has been used for all the PD's that we fabricated. Further experiments will be performed on the guard ring structure. The ring width, the distance between the ring, and the collector electrode, will be varied systematically to find that geometry which best reduces the detector leakage current.

Asymmetric detector geometries with a larger top contact and a smaller bottom contact (instead of equal contact areas) are being considered to reduce the detector capacitance, while maintaining as large as possible the photon collection area. These geometries will be evaluated with new detectors.

#### d) Encapsulation and packaging

We have developed a specialized way to ruggedly package the HgI<sub>2</sub> detector. In the construction, the HgI<sub>2</sub> crystal is securely mounted onto a robust ceramic substrate with the front entrance covered by a quartz window. Most detectors made during the phase I period were encapsulated with only silicone rubber. In order to best utilize our limited supply of materials, it was necessary to refabricate some detectors to various thicknesses and sizes. For those cases, we found that detectors coated with silicone rubber were more easily repolished and refabricated. A combination of silicone rubber and Parylene coating has been used for detector encapsulation in the phase II period. The Parylene coating ensures detector stability and reliability under vacuum and other demanding ambient conditions. Two legs on both sides of the detector fully support the quartz front cover; any mechanical forces introduced during optical coupling and decoupling operations to the scintillator crystal are thus removed from the fragile region of the front electrode/HgI<sub>2</sub> surface. Stresses in this new configuration were instead transferred to the sturdy support legs and quartz window. However, it is difficult to make the height of the legs exactly the same as the thickness of the HgI<sub>2</sub> crystal plus the hydrogel contact (i.e., the distance between the window and the substrate) with the result that the possibility for some stress to the detector still remains. We are planning to use springs to support the entrance window instead of solid legs. This configuration will remove most mechanical forces introduced during optical coupling and decoupling operations as well as due to the weight of the scintillator.

#### e) Electrical and optical tests

Each fabricated HgI<sub>2</sub> PD has been tested in combination with a scintillator (CsI(Tl)), using standard NIM counting electronics. The energy resolution of each scintillator/HgI<sub>2</sub> spectrometer pair was measured for 662 keV gamma rays from <sup>137</sup>Cs. Some of the PD's have been tested coupled to scintillators of various sizes and shapes. Various radiation sources were also used.

Leakage currents have been measured for 0.5" detectors. Further measurement will be done on larger size detectors (e.g., 1" and larger detectors). The quantum efficiency of HgI<sub>2</sub> PD's at various wavelengths will be measured using the facility at Advanced Photonics. Photoresponse spatial maps over the detector's entrance electrode regions are

also planned to determine the uniformity, surface condition and photoelectric properties of the crystal.

f) Temperature/vacuum/radiation tests

The electrical and optical measurements mentioned above will be repeated at various temperatures. The detectors will be tested under vacuum for a period of time. The radiation damage test in space originally was planned with Dr. Penny Haskins at the Institute for Space Science and Technology. However, because of the shortage of funding, the plan has been canceled for the near future. The opportunity for detector radiation damage measurement in accelerator facilities will be researched.

2) Development of HgI<sub>2</sub>/scintillator gamma detector (on schedule)

a) Optical/mechanical coupling study

A literature study and measurement research have been done on the optimization of CsI(Tl)/HgI<sub>2</sub> gamma-ray detectors. The optimal match between scintillators and PD's was studied. In order to study the use of light guides to couple large diameter scintillators with smaller active area PD's, measurements were done using a 0.6" diameter Avalanche Photodiode (APD) coupled to a 1"x1" cylindrical scintillator (CsI(Tl)). First, a Plexiglas taper was used as a light pipe between the APD and the scintillator. This taper (0.047" long) was made with flat, circular end surfaces, one of 0.6" diameter and the other 1" diameter. The smaller end matches the APD, while the larger end matches the 1" scintillator. The side surface of this taper was wrapped with Teflon tape and aluminum foil as the reflector. Second, the APD was directly coupled to the glass window of the scintillator. The area of the scintillator window not covered by the APD was covered by Teflon tape and aluminum foil. The light collection was compared by measuring the peak position with the viewed light output. The measurement result showed that the total efficiency of the second configuration (direct coupling) was increased about 50% over the result from the first configuration (taper). Therefore, this configuration was used for later measurement. However, according to [1] when a tapered scintillator was used with a smaller photodiode (instead of using a tapered light pipe between the larger scintillator and the smaller photodiode), higher light collection efficiency was obtained over the latter configuration. The tapered scintillator will be evaluated with our PD.

The light collection (HgI<sub>2</sub> PD coupled to CsI(Tl)) of different sizes and shapes was also compared. A 0.5" HgI<sub>2</sub> PD was coupled to 0.5"x0.5" cylindrical and 1"x1"x1" cube CsI(Tl) scintillators, respectively. The total efficiency of the cylindrical scintillator was about 90% higher than the cube scintillator. This is likely due to the trapping of light in the sharp edges of the cube crystal, hence the total efficiency dropped significantly. A further study will be done to optimize the geometry of the scintillator for a multi-detector system.

## b) Resolution vs. scintillator type and size

In order to study how the size of the scintillator affects the energy resolution of the spectrometer, a 0.5" PD was tested with a 0.5"x0.5" CsI(Tl) and then a 1.5"x1.5" CsI(Tl) scintillator was tested with the same 0.5" PD. The second scintillator has a larger output window than the active area of the PD. Reflective and light-tight materials (Millipore filter paper, Teflon tape and aluminum foil) were used to cover the area of the scintillator window that was not covered by the PD. The central 0.5" diameter of the scintillator was coupled to the PD through a thin quartz coupler. Figure 1 shows the comparison between spectra taken with the 0.5" HgI<sub>2</sub> PD coupled to 0.5"x0.5" and coupled to 1.5"x1.5" scintillators, respectively. The solid line spectrum was taken with the 0.5"x0.5" scintillator while the dotted line spectrum was taken with the 1.5"x1.5" scintillator. The photofraction of the spectrometer was improved from 17% (0.5"x0.5" scintillator) to 38% (1.5"x1.5" scintillator). The spectrum from the 0.5"x0.5" scintillator shows better FWHM resolution, 4.8%, compared to 6.4% FWHM resolution from the 1.5"x1.5" scintillator. However, the spectrum from the 1.5"x1.5" scintillator shows much higher detection efficiency than from the 0.5"x0.5" scintillator (i.e., much higher peak-to-Compton ratio in the spectrum). The broader photopeak was due to statistical degradation due to poor light collection from the larger crystal. Nevertheless, this result is very encouraging. Changing the size of the scintillator from 0.5" diameter to 1.5" diameter with the same 0.5" HgI<sub>2</sub> PD caused the energy resolution to only deteriorate from 4.80% to 6.40%. The 0.5" PD was also tested with 0.5"x0.5" CsI(Tl) and 1"x1"x1" (cube) CsI(Tl) scintillators. The energy resolution at 662 keV from <sup>137</sup>Cs was measured to be 4.75% when the detector was coupled to the 0.5"x0.5" scintillator; the resolution was measured to be 8.27% when coupled to the 1"x1"x1" scintillator. The relatively poor resolution from the cube scintillator was caused by the poor light collection due to the scintillator geometry.

The gamma response linearity (over the energy range of 60 to 1332 keV) of HgI<sub>2</sub>/CsI(Tl) coupling configuration was measured using HgI<sub>2</sub> PD N15-2F1, coupled to a 0.5"x0.5" CsI(Tl) scintillator. Various radiation sources, <sup>241</sup>Am, <sup>133</sup>Ba, <sup>109</sup>Cd, <sup>57</sup>Co, <sup>22</sup>Na, <sup>137</sup>Cs, <sup>54</sup>Mn and <sup>60</sup>Co, were used. The centers of the photopeaks for these various sources were plotted as a function of source energy and are shown in Figure 2. These data show that the response of the PD is linear with scintillator light intensity. The energy resolution was also measured with various radiation sources. Figure 3 shows the spectrum of <sup>22</sup>Na source for a 0.5" CsI(Tl) crystal coupled to HgI<sub>2</sub> PD N15-2F1. The energy resolution for the 511 keV photopeak is 6.78% (FWHM). Figure 4 shows the spectrum of <sup>60</sup>Co source for the same CsI(Tl)/HgI<sub>2</sub> pair and the energy resolution for the 1332 keV photopeak is 3.20%.

We will next test the detector's performance vs. temperature and the detector's long term stability and reliability.

### 3) Electronics development (on schedule)

#### a) Low noise amplification circuits

In the past, optimized charge-sensitive preamplifiers have been designed by Xsirius for use with  $\text{HgI}_2$  x-ray detectors. Compared to x-ray detectors,  $\text{HgI}_2$  PD's have larger capacitance because of their larger areas. In order to get the best results, some tests were performed using modified preamplifiers. More specifically, different preamp input FETs were investigated in order to optimize parameters for the larger input capacitance of the PD's. The best results were obtained with type U311 FET's from InterFET Corporation. The U311 FET was used for our testing chamber. The search for new FET's suitable for our large-area PD's will be continued.

The main amplifier used was Tennelec 244. The longest peaking time available of this amplifier is 24  $\mu\text{s}$ . The decay constant ( $1/e$ ) of  $\text{CsI(Tl)}$  is 1  $\mu\text{s}$  which is relatively long compared to the decay constant of other scintillators. In order to fully collect the scintillation light, longer peaking times should be used. One Tennelec 244 was modified to increase the peaking time to about 45  $\mu\text{s}$ ; the best energy resolution was obtained with this peaking time. The energy resolution vs. peaking time was measured using a 0.5" PD coupled to a 0.5"x0.5" scintillator. The FWHM for 662 keV gamma-ray from  $^{137}\text{Cs}$  were measured as:

Peaking time ( $\mu\text{s}$ )	FWHM at 662 keV
16	5.46%
24	5.25%
45	5.10%

#### b) Coincidence circuit

In order to maximize the signal, minimize the noise contribution in the gamma spectra, and improve the overall system resolution, a coincidence technique is used for the multi-detector system. A logic circuit has been designed and built to realize this for a two detector system.

The front-end of the system is formed using low-noise, low-power, hybridized charge sensitive preamplifiers. Signals from the preamplifiers, after pole-zero cancellation, are fed to the inputs of the shaping amplifiers. The amplifiers that we used (i.e., Tennelec model TC244) provided separate outputs for unipolar and bipolar signals. The bipolar signal was derived from the unipolar signal by simple differentiation. Both output signals were used for the coincidence circuit. The unipolar outputs were used as the real signals and the bipolar outputs were used as references to determine if the events occurred in coincidence.

We tried different schemes to combine the signals from the shaping amplifiers which are the result of a single event that has been detected in coincidence by two detectors. The finalized circuit is shown in Figure 5. The technique we used is based on

straightforward summation of two unipolar output signals. In order to improve the signal-to-noise ratio, we used relatively long shaping times (12 $\mu$ s). The pulse shape is almost triangular. At such a long shaping time, we achieved a close matching of signals from the two amplifiers within a very broad range of input count rates and signal amplitudes.

In the control path we used signals coming from the bipolar outputs of the TC244 amplifiers. The noise level from the bipolar output is higher than that from the unipolar output, due to the signal differentiation. The bipolar signal is still an excellent reference source for timing purposes. These bipolar signals, when coming in coincidence from the two sources within the specified timing window, trigger a GATE signal to the MCA which allows MCA to process signal from the summing channel.

A one inch cube CsI(Tl) scintillator with two windows (0.5" diameter) opened at two adjacent surfaces was coupled to two 0.5" PD's (V5-6F1 and N15-2F1). The coincidence circuit (described in Figure 5) was used to combine (sum) the signals from both PD's of this two-detector configuration. Energy resolutions of each single detector and combined configuration were compared. The FWHM resolutions of the photopeaks (662 keV) were 8.69% and 8.28% for detectors V5-6F1 and N15-2F1, respectively. The poorer resolutions (compared to 4.80% and 4.75%, respectively, when these two detectors were coupled to a 0.5"x0.5" CsI(Tl) scintillator) are due to the scintillator itself. The reasons for this include the broadening due to local fluctuations in the scintillator uniformity, the geometry, and the surface conditions. The FWHM of the overall photopeak was 6.56%. This improved result of the summation of these two detectors with the coincidence circuit is encouraging and shows a useful approach to matching the PD's to large scintillators. In addition, the geometry of the scintillator and PD mounting configuration could be improved further to optimize the light collection from large scintillators and hence improve the overall performance of the spectrometer.

We will next design and build the anticoincidence circuits.

#### 4) Gamma instrument prototype (initiated in 6th quarter)

This part of the works include active shield/APD experimentation and assembly of the demonstration unit. The final tests will be performed in our lab with different radiation sources.

The active shield/APD experiment started with the selection of optimal scintillators coupled with APD's. In order to do this, an APD (200 mm<sup>2</sup>) made by Advanced Photonics was tested with different scintillators and radiation sources. Figure 6 shows spectra of <sup>137</sup>Cs and <sup>241</sup>Am sources for a 0.5" CsI(Tl) crystal coupled to the 200 mm<sup>2</sup> APD. The energy resolutions are 6.05% (FWHM) and 22.4% (FWHM) for 662 keV and 59.6 keV, respectively. The Ba 32 keV x-ray peak is also pronounced in the spectrum. A spectrum of a <sup>137</sup>Cs source measured by the APD coupled to a NaI(Tl) scintillator is shown in Figure 7. An energy resolution of 7.7% was obtained. Figure 8 presents a spectrum of a



$^{22}\text{Na}$  source obtained from a BGO with the APD. The energy resolution of the 511 keV photopeak is 14% FWHM.

#### Reference

[1] A.J. Bird, T. Carter, A.J. Dean, D. Ramsden and B.M. Swinyard, "The Optimization of Small CsI(Tl) Gamma-ray Detectors," IEEE Tran. on Nucl. Sci. Vol. 40, No. 4, August 1993.



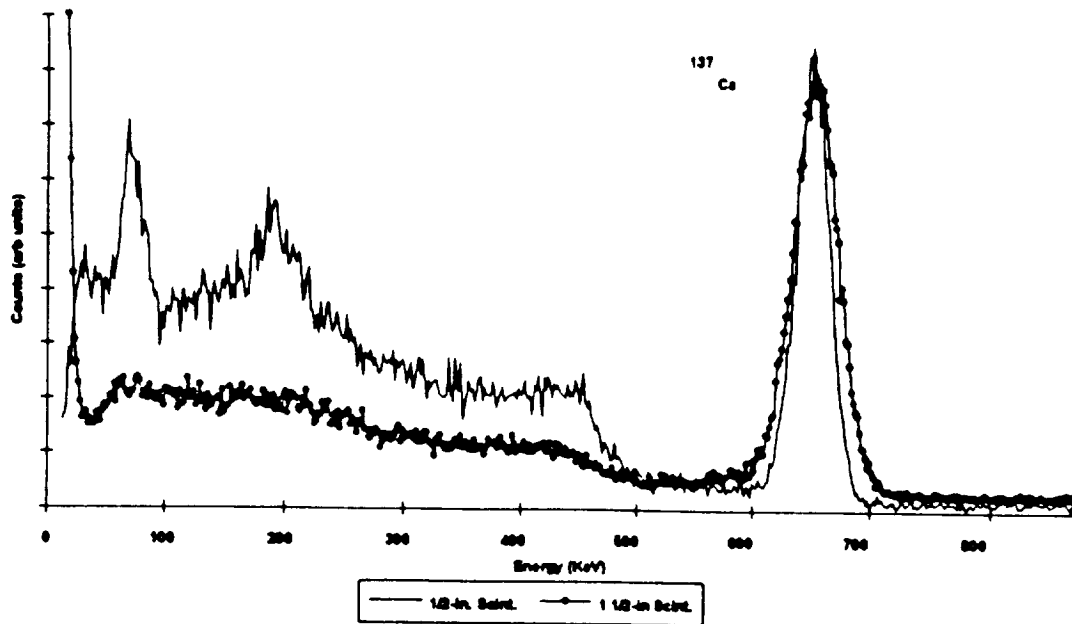


Figure 1 Spectra taken with a 0.5" HgI<sub>2</sub> photodetector coupled to a 0.5"x0.5" CsI(Tl) (solid line, FWHM: 4.80%) and to a 1.5"x1.5" CsI(Tl) (dotted line, FWHM: 6.40%) for gamma rays from a <sup>137</sup>Cs source.

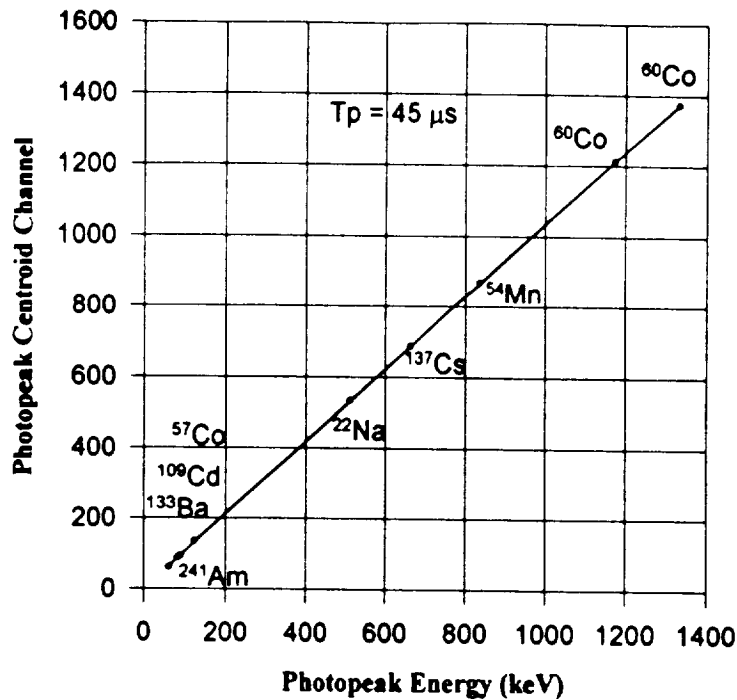


Figure 2 Gamma response linearity of a 0.5" HgI<sub>2</sub> photodetector coupled to a 0.5"x0.5" CsI(Tl) scintillator. Radiation source <sup>241</sup>Am, <sup>133</sup>Ba, <sup>109</sup>Cd, <sup>57</sup>Co, <sup>22</sup>Na, <sup>137</sup>Cs, <sup>54</sup>Mn and <sup>60</sup>Co were used.

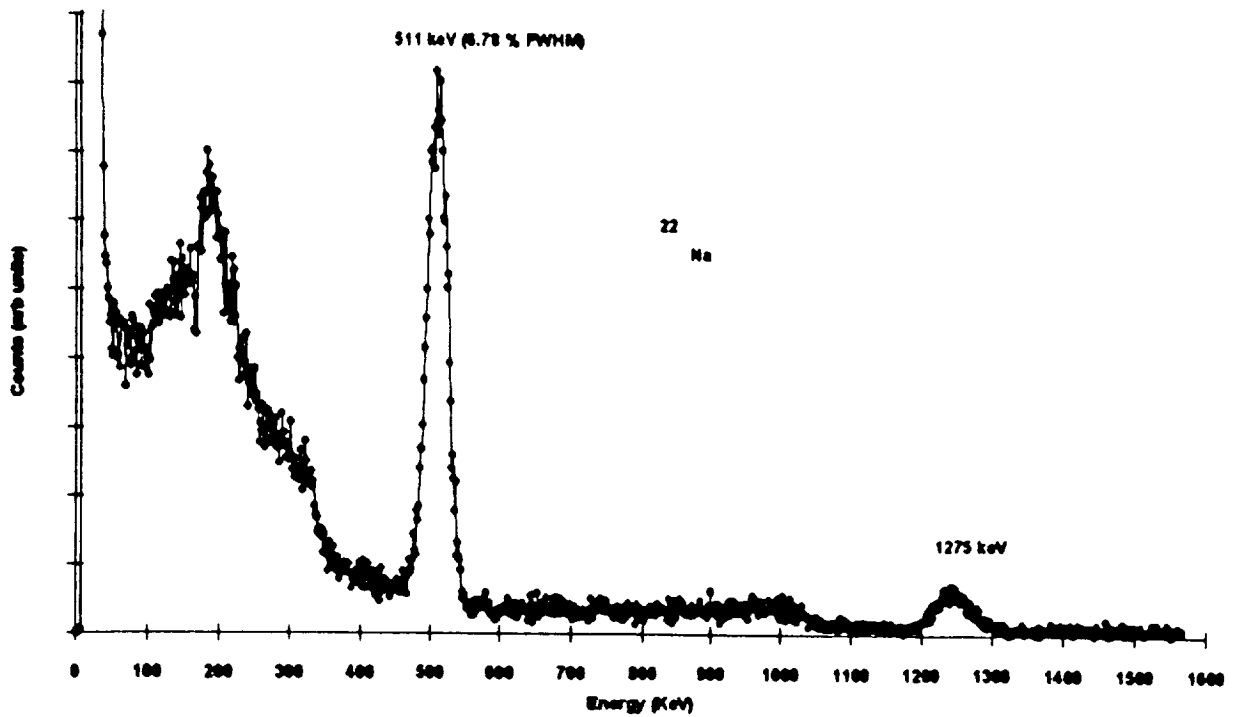


Figure 3. The spectrum taken with a 0.5"  $\text{HgI}_2$  photodetector coupled to a 0.5"x0.5"  $\text{CsI(Tl)}$  scintillator for gamma rays from a  $^{22}\text{Na}$  source. The FWHM energy resolution for 511 keV is 6.78%.

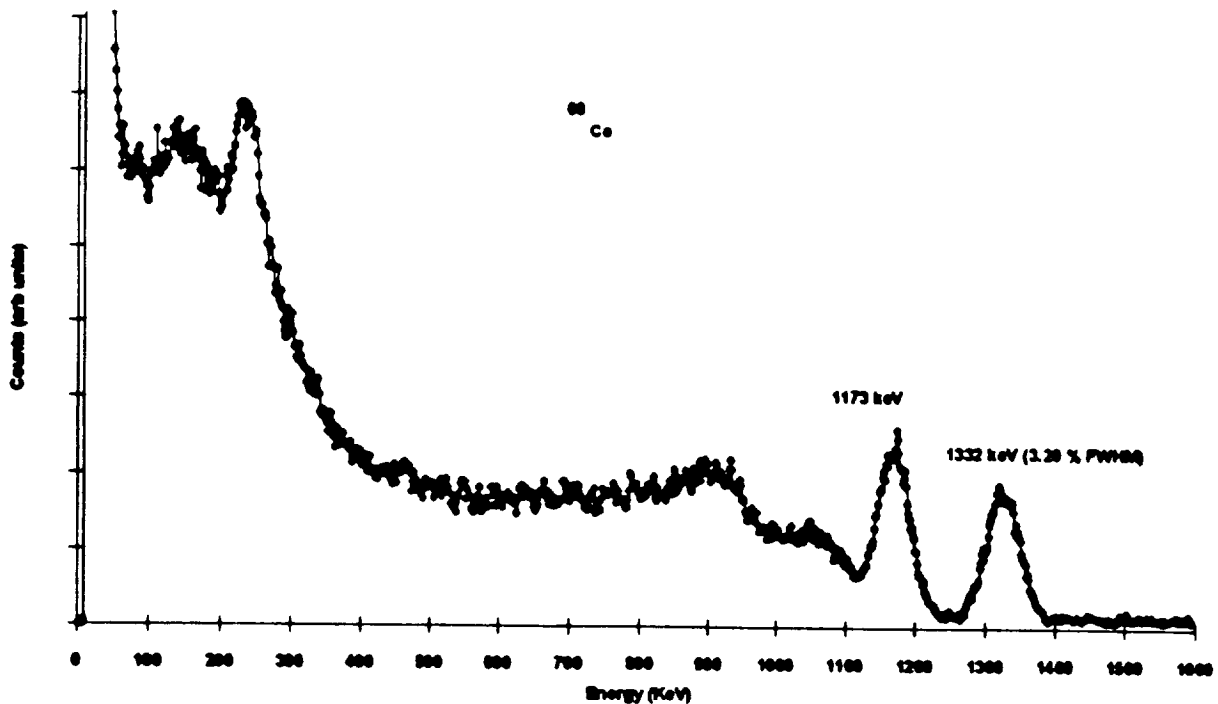


Figure 4. The spectrum taken with the same  $\text{CsI(Tl)}/\text{HgI}_2$  pair as shown in figure 3 for gamma rays from a  $^{60}\text{Co}$  source. The FWHM energy resolution for 1332 keV is 3.20%.



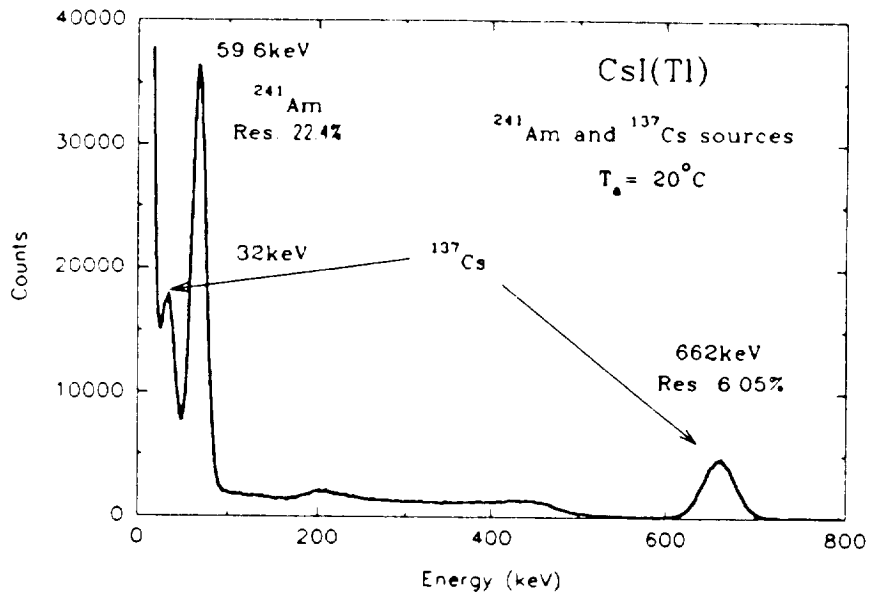


Figure 6. Energy spectrum of the  $^{137}\text{Cs}$  and  $^{241}\text{Am}$  sources obtained with a  $200\text{ mm}^2$  APD on a CsI(Tl) scintillator.

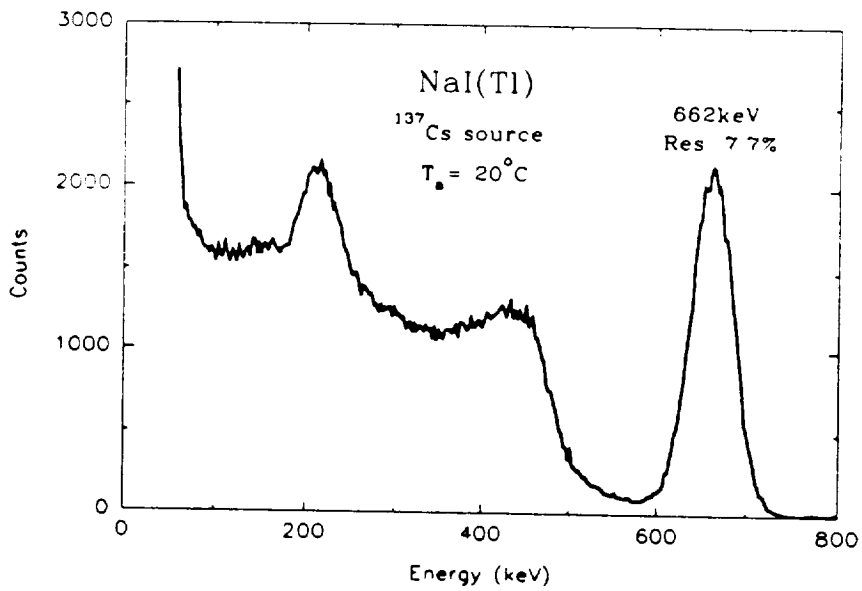


Figure 7. Energy spectrum of the  $^{137}\text{Cs}$  source obtained with a  $200\text{ mm}^2$  APD on a NaI(Tl) scintillator.

V180130.DAT BGO + Na-22  
Res. (511) =  
APD: 18-01

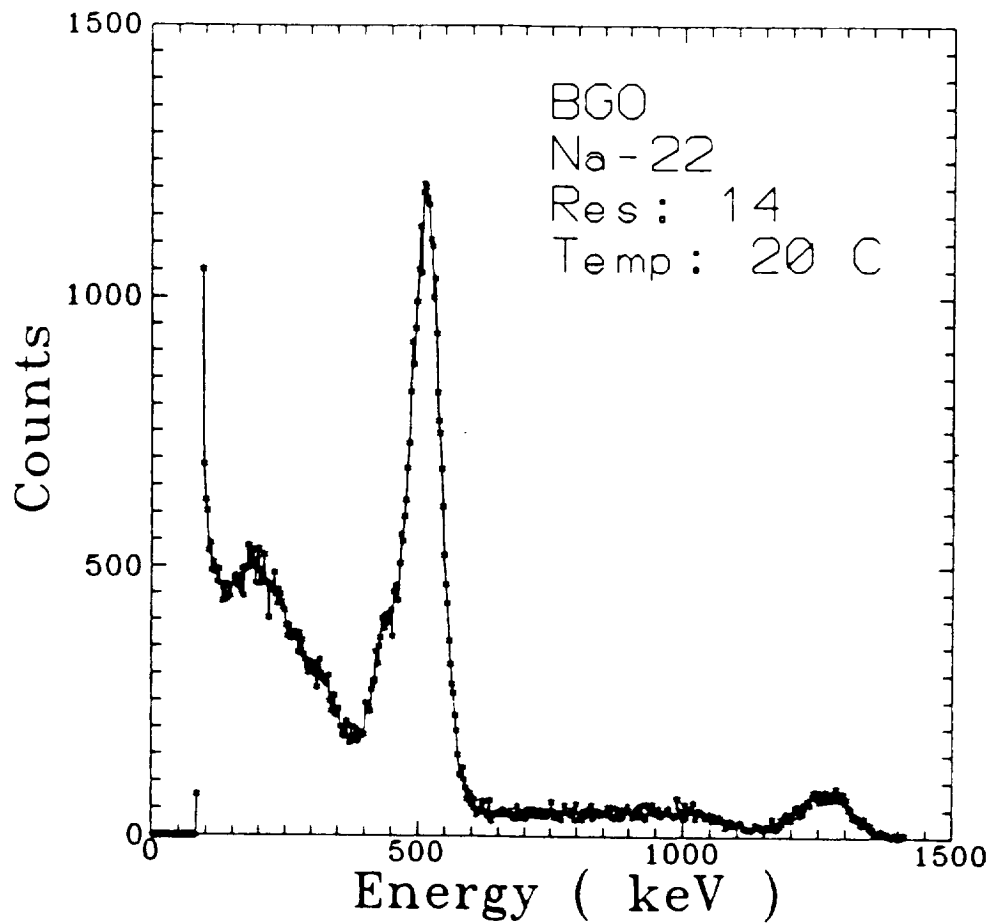


Figure 8. Energy spectrum of the  $^{22}\text{Na}$  source obtained with a  $200\text{ mm}^2$  APD on a BGO scintillator.